PEIERLS BARRIER - NABARRO AND MIGRATION MONOVACANCIES AND MULTIVACANCIES IN GRAPHENE

Yurov V.,
Candidate of Physics and Mathematics Sciences, Associate Professor
KarTU, Karaganda, Kazakhstan
Zhangozin K.
Candidate of Physics and Mathematics Sciences, Associate Professor,
TSK Vostok LLP, Ust-Kamenogorsk, Republic of Kazakhstan
https://doi.org/10.5281/zenodo.10515013

Abstract
In the article, we compare a graphene monolayer with the Peierls–Nabarro barrier, which is equal to the force of interatomic interaction. This barrier is calculated from the formation energy of monovacancies, divacancies and other structural defects and the length of the newly formed carbon bond. It is shown that the Peierls–Nabarro barrier is maximum for a monovacancy and then decreases for complex defects.

Keywords: graphene, monolayer, monovacancy, divacancy, defect, carbon, barrier, dislocation.

Introduction

Defects and impurities have a significant impact on the mechanical, electrical, optical and other properties of solids, and, in particular, graphene, discovered at the beginning of the 21st century [1]. Graphene has two types of defects: (i) natural defects known as intrinsic defects in graphene, such as Stone–Wells defects, single vacancy defects, multiple defects, linear defects, and carbon adatoms; and (ii) physically introduced defects, known as extrinsic defects in graphene, which are foreign adatoms and foreign impurities [2-4].

In this article, we will consider the effect of monovacancies and multivacancies on the physical properties of graphene. Then we compare the energy of their formation and migration with the Peierls–Nabarro barrier in graphene.

Monovacancy in graphene

A monovacancy (SV) or Schottky defect is the absence of an atom or ion at a site in a crystal lattice. A monovacancy (SV) was experimentally observed in graphene in [4-7] and its image is shown in Figure 1.

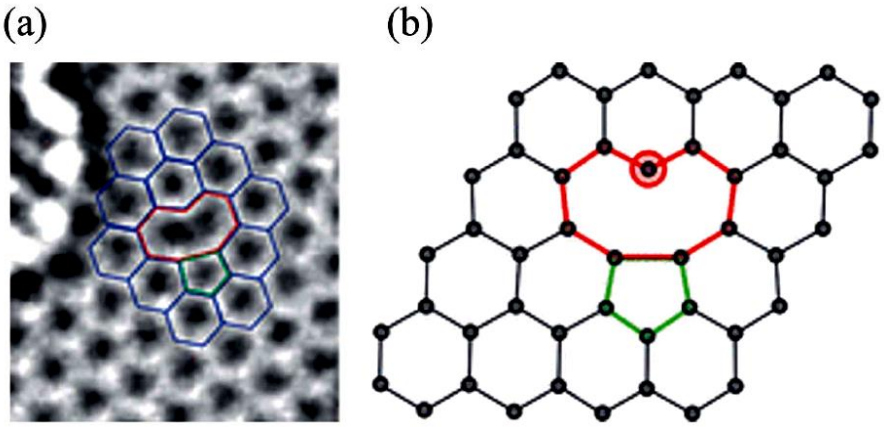

Figure 1. Monovacancy in graphene: experimental TEM image (a); atomic structure obtained as a result of calculations using the DFT method (b) [4].

Calculations have shown that the local threefold symmetry of graphene D_{3h} is broken to the C_{2v} symmetry due to the Jahn-Teller distortion [8-11]. A monovacancy has a 5/9 structure, where a new bond with length b_{CV} arises between a pair of three atoms with dangling bonds, forming a pentagon with a displacement d_{CV} of the third atom from the graphene plane [2, 12-14]. This moment is depicted in Figure 2. The energy of formation of monovacancies is E_{CV} = 7.6-7.9 eV and the length of the newly formed bond is b_{CV} = 0.18 - 0.2 nm, the migration barrier is ΔE_{CV} = 1.3 eV at 100 - 200 °C and out-of-plane movement d_{CV} = 0.018 nm [4, 8-10]. If we take the average values of E_{CV}, ΔE_{CV} and energy converted into joules, we get E_{CV} = 12.4 10^{-19} N/m, ΔECV = 2.1 10^{-19} J = 2.1 10^{-19} N/m. The force of formation of monovacancies is equal to $F_{CV} = E_{CV}/b_{CV}$ = 12.4 10^{-19} N/m/1.9 10^{-10} m = 6.5 10^{-9} N, The force of movement of the migration barrier is equal to $\Delta F_{CV} = \Delta E_{CV}/d_{CV}$ = 2.1 10^{-19} N/m/0.18 10^{-10} m = 11.7 10^{-9} N.

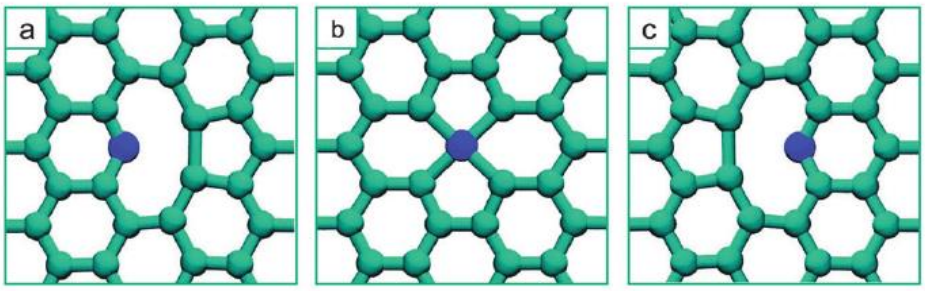

Figure 2. Initial ground state (a), transition state (b) and final ground state (c) for one step of migration of a reconstructed 5/9 monovacancy into graphene [2].

Divacancy in graphene

A double vacancy (DV) means either the fusion of two single vacancies (SV) or the removal of two adjacent carbon atoms. The DV can be reconstructed to produce two pentagons and one octagon, indicated by the 5-8-5 defect [15, 16]. Figure 3 shows the atomic structure of divacancies obtained by DFT and experimental images obtained by TEM.

The formation energy of DV is equal to E_{DV} = 7.5 eV and is less than that of SV, the length of the newly formed bond is bDV = 0.17 nm. The transformation barrier values for the transition 5-8-5 → 555-777 are 5.17 - 5.27 eV [8, 9]. All three divacancy states are stable at room temperature.

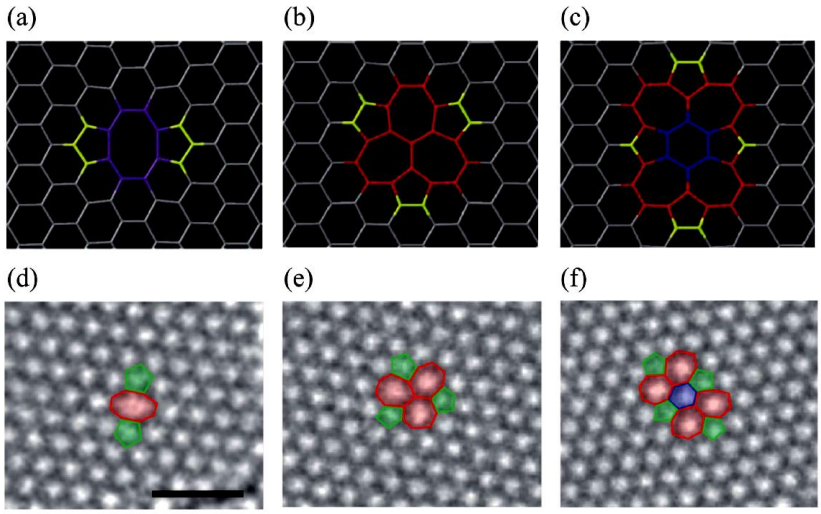

Figure 3. Divacancy in graphene. Atomic structures obtained from DFT calculations (a-c). Experimental TEM images corresponding to atomic models (d-f). Here defect 5–8–5 (a, d), defect 555–777 (b, e) defect 5555–6–7777. (c, f) [4].

The DV defect is caused by a dangling bond, whereas the 5–8–5 defect causes only local deformations. Being a saturated eight-membered ring compound, the cyclooctane $(CH_2)_8$ molecule also has a nonplanar structure. resembling a crown or a boat. Since defect 5–8–5 also has significant local curvature, the system is replaced with defect 555–777 or 5555–6–7777 to reduce local curvature. Three different reconstructed states of divacancy in graphene are usually observed in it under electron irradiation (Figure 4).

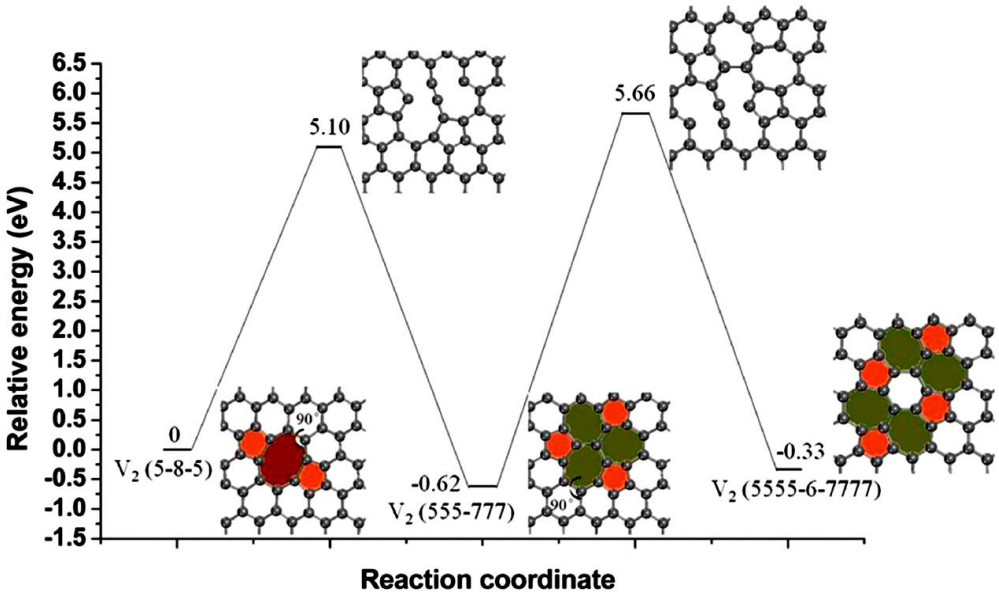

Figure 4. Schematic representation of the structure and energetics of three divacancy states in graphene: the V_2(5-8-5) state, the V_2(555-777) state, and the V_2(5555-6-7777) state and the transition states for the transition between the V_2(states 5-8-5) and V_2(555-777) and between the states V_2(555-777) and V_2(5555-6-7777) [2].

Multivacancies in graphene

The removal of more than two carbon atoms, known as multiple defects or multivacancies, can result in a larger, more complex defect. In this regard, one would expect to observe a more or less random selection of vacancies. Therefore, local rearrangement of the lattice around multivacancies and the formation of a random set of non-hexagonal polygons is possible. Two pentagons and one octagon appear for the reconstructed double vacancy, resulting in the absence of dangling bonds [17]. Multivacancies can be created by modern physical and chemical methods [18-21]. Research results show that multivacancies are more easily formed than monovacancies under electron irradiation [22]. Calculations show that the energy of formation of multivacancies in graphene and carbon nanotubes is significantly lower than the energy of formation of monovacancies [23-26]. The formation energy of the 5555–6–7777 defect is between 5–8–5 and 555–777 (Fig. 4) and is about 6 eV with a bond length of about 0.23 nm [27, 28].

Peierls–Nabarro barrier

In [29], our proposed model of the surface layer of atomically smooth metals is generalized. To determine the thickness of the surface layer of various compounds, the size dependence of the melting temperature $T_m(r)$ was used:

$$\begin{aligned} T_m(r) &= T_m(\infty)\cdot\left(1-R(I)/r\right), \qquad r >> R(I), \\ T_m(r) &= T_m(\infty)\cdot\left(1-R(I)/R(I)+r\right), \quad R(0) \le r \le R(I). \end{aligned} \tag{1}$$

Here the first formula coincides with the formula of R. Tolman [30], where $R(I) = 2\delta$, δ is the Tolman parameter, which is not determined experimentally. The second formula is further defined in the region $R(0) < r < R(I)$, so that when $r = 0$ the first formula does not go to infinity. The parameter R(I) is related to the surface energy γ by the formula [29]:

$$R(I) = 2\gamma\upsilon/RT\,. \tag{2}$$

Here γ is the surface energy of the massive sample; υ – volume of one mole; R – gas constant; T – temperature. In [31] it is shown that, with an accuracy of 3%, the following is true:

$$\gamma = 0{,}70\cdot 10^{-3}\cdot T_m \ \ [J/m^2], \tag{3}$$

where T_m is the melting temperature of the solid (K). The relationship holds for all metals and for other crystalline compounds. At $T = T_m$ from (2) we obtain:

$$R(I) = 0{,}17\cdot 10^{-9}\upsilon \ \ (m). \tag{4}$$

Equation (4) shows that the thickness of the surface layer R(I) is determined by one parameter – the molar (atomic) volume of the element ($\upsilon = M/\rho$, M – molar mass (kg/mol), ρ – density (kg/m3)) , which changes periodically in accordance with table D.I. Mendeleev.

We compare the R(I) monolayer with the Peierls–Nabarro barrier, which is equal to the force of interatomic interaction [32, 33]. In contrast to the Frenkel–Kontorova model [34], as well as works [35, 36] and others, we will propose a model that can be used to estimate the barrier $F(I)_{P\text{-}N}$ and voltage $\sigma(I)_{P\text{-}N}$ the Peierls – Nabarro:

$$\begin{aligned} F(I)_{P\text{-}N} &= \gamma\cdot R(I)/n = \gamma\cdot a, \\ \sigma(I)_{P-N} &= F(I)_{P-N}/S = \gamma/a = E\cdot\varepsilon(I), \end{aligned} \tag{5}$$

where n is the number of layers in layer R(I); a is the lattice constant; S – barrier area (a^2), $\sigma(I)_{P\text{-}N}$ – Peierls–Nabarro stress; E – Young's modulus; ε represents the relative elongation of the lattice parameter in the direction of the external force F. In the case of graphene, R(I) = a = 0.246 nm, n = 1, γ = = 3157 mJ/m^2.

Peierls–Nabarro barrier and parameters of vacancies in graphene

Using equations (1) – (5), we calculate the energy parameters of graphene and vacancies in graphene (Table 1).

Table 1.

Parameters of graphene and vacancies in graphene

Parameter	$F(I)_{P-N}$, 10^{-9} N	$\sigma(I)_{P-N}$, MPa	F_{CV}, 10^{-9} N	$\sigma(I)_{CV}$, MPa	F_{DV}, 10^{-9} N	$\sigma(I)_{DV}$, MPa	F_{D}, 10^{-9} N	$\sigma(I)_{D}$, MPa
Graphene	0,26	4268	-	-	-	-	-	-
Monovacancy	-	-	0,65	36111	-	-	-	-
Divacancy	-	-	-	-	0,44	25872	-	-
Defect 5555–6–7777	-	-	-	-	-	-	0,26	11304

From Table 1 it follows that the Peierls–Nabarro stress for pure graphene is $\sigma(I)_{P-N}$ = 4.3 GPa and then decreases with increasing number of defects. This value of the Peierls–Nabarro stress leads to warping of sheets of pure graphene [2, 37]. In graphene, the deformation σ(I) of the quasi-two-dimensional lattice created by the defects listed above can induce strong pseudomagnetic fields, promote the appearance of new Landau levels and paramagnetic centers, and have a significant impact on the electronic characteristics [38–43]. From Table 1 it follows that the Peierls-Nabarro barrier for pure graphene is $F(I)_{PN} = 0.26\ 10^{-9}$ N, and for typical steel $F(I)_{P-N} = 0.5\ 10^{-9}$ N. A monovacancy has a large Peierls barrier – Nabarro, although they are not easy to form. The Peierls–Nabarro barrier inhibits the movement of dislocations in metals and leads to its strengthening [44]. Defects in graphene, which can inhibit the movement of dislocations, are more easily formed under electron irradiation [22].

The displacement of monovacancies outside the graphene plane is (see above) d_{CV} = 0.018 nm and, therefore, d_{DV} = 0.027 nm and d_D = 0.046 nm (see Table 1). In [45], the formation and movement of dislocations in graphene was studied in real time using high-resolution transmission electron microscopy. It was established in [45] that the source of dislocations in graphene are the so-called Stone-Wales defects, which are formed as a result of rotation of the C–C bond through an angle of 90°, as a result of which two pentagons and two heptagons appear in the hexagonal lattice. Dislocations move by sliding or crawling at a speed of ~ 0.1 nm/min. Each dislocation creates a deformation field in its vicinity, which extends over ~ 1 nm.

Conclusion

Today, there are several mechanisms of dislocation braking, which can be divided into two groups. The first group discusses the inhibition of dislocations due to the presence of potential barriers in crystals caused by various structural defects, including the Peierls–Nabarro barrier. The second group discusses the inhibition of dislocations due to the presence of dynamic interaction in crystals. This includes interaction with electrons, phonons, excitons, magnons and other elementary excitations of the crystal lattice. The role of the latter excitations is insignificant for most crystals, but the interaction with phonons is most significant. As we have shown, the Peierls–Nabarro barrier in graphene is maximum for a monovacancy.

References:

1. Novoselov K.S. Graphene: materials from Flatland // UFN, 2011, Vol. 181, No. 12. - P. 1299-1311.

2. Skowron S.T., Lebedeva I.V., Popovc A.M. and Bichoutskaia E. Energetics of atomic scale structure changes in grapheme // Chem. Soc. Rev., 2015, V. 44. – P. 3143-3176.

3. Wu J.-B., Lin M.-L., Cong X., Liu H.-N. and Tan P.-H. Raman spectroscopy of graphene-based materials and its applications in related devices // Chem. Soc. Rev., 2018, V. 47, - P. 1822-1873.

4. Bhatt M.D., Kim H. and Kim G. Various defects in graphene: a review // RSC Adv., 2022, V. 12. – P. 21520–21547.

5. Gass M.H., Bangert U., Bleloch A.L., Wang P., Nair R.R. and Geim A. Free-standing graphene at atomic resolution // Nat. Nanotechnol., 2008, 3, 676–681.

6. Meyer J.C., Kisielowski C., Erni R., Rossell M.D., Crommie M. and Zettl A. Direct imaging of lattice atoms and topological defects in grapheme membranes // Nano Lett., 2008, 8, 3582–3586.

7. Yazyev O.V. and Helm L. Defect-induced magnetism in graphene // Phys. Rev. B: Condens. Matter Mater. Phys., 2007, V. 75, 125408.

8. El-Barbary A.A., Telling R.H., Ewels C.P., Heggie M.I. and Briddon P.R. Structure and energetics of the vacancy in graphite // Phys. Rev. B: Condens. Matter Mater. Phys., 2003, V. 68, 144107.

9. Krasheninnikov A.V., Lehtinen P.O., Foster A.S. and Nieminen R.M. Bending the rules: Contrasting vacancy energetics and migration in graphite and carbon nanotubes // Chem. Phys. Lett., 2006, V. 418. – P. 132-136.

10. Saito M., Yamashita K. and Oda T. Structures and Electronic Properties of Graphene with Vacancy Defects // Jpn. J. Appl. Phys., 2007, V. 46. - L1185-1187.

11. Nanda B.R.K., Sherafati M., Popovicr Z.S. and Satpathy S. Electronic structure of the substitutional vacancy in graphene: Density-functional and Green's function studies // New J. Phys., 2012, V. 14, 083004.

12. Robertson A.W., Montanari B., He K., Allen C.S., Wu Y.A., Harrison N.M., Kirkland A.I. and Warner J.H. Dynamics of Single Fe Atoms in Graphene Vacancies // ACS Nano, 2013, V. 7. – P. 4495-4502.

13. Latham C.D., Heggie M.I., Alatalo M., Oëberg S.O. and Briddon P.R. The contribution made by lattice vacancies to the Wigner effect in radiation-damaged graphite // J. Phys.: Condens. Matter, 2013, V. 25, 135403.

14. Trevethan T., Latham C.D., Heggie M.I., Briddon P.R. and Rayson M.J. Vacancy diffusion and coalescence in graphene directed by defect strain fields // Nanoscale, 2014, V. 6. – P. 2978-2986.

15. Liu L. and Chen S. Geometries and Electronic States of Divacancy Defect in Finite-Size Hexagonal Graphene Flakes // Journal of Chemistry, 2017, 8491264.

16. Zare1 M. and Asgari R. Probing divacancy defects in a zigzag graphene nanoribbon through RKKY exchangeinteraction // J. of Physics D Applied Physics, 2020, V. 54(9). – P. 1-11.

17. Ugeda M.M., Brihuega I., Hiebel F., Mallet P., Veuillen J.-Y., Gormez-Rodrıгguez J.M. and Yndurrain F. Electronic and structural characterization of divacancies in irradiated graphene // Phys. Rev. B: Condens. Matter Mater. Phys., 2012, V. 85, 121402.

18. Hou Z. and Terakura K. Effect of multiple defects and substituted impurities on the band structure of graphene: a DFT study // J. Phys. Chem. C, 2015, V. 119. – P. 4922-4933.

19. Rodrigo L., Pou P. and Perrez R. Graphene monovacancies: Electronic and mechanical properties from large scale ab initio simulations // Carbon, 2016, V. 103. – P. 200–208.

20. Hirunsit P., Liangruksa M. and Khanchaitit P. Electronic structures and quantum capacitance of monolayer and multilayer graphenes influenced by Al, B, N and P doping, and monovacancy: Theoretical study // Carbon, 2016, V. 108. – P. 7-20.

21. Asadov M.M., Mustafaeva S.N., Guseinov S.S., Lukichev V.F. Ab Initio Calculations of the Electronic Properties and the Transport Phenomena in Graphene Materials // Phys. Solid State, 2020, V. 62, № 11. - P. 2224–2231.

22. Hashimoto A., Suenaga K., Gloter A., Urita K. and Iijima S. Direct Evidence for Atomic Defects in Graphene Layers // Nature, 2004, V. 430. - P. 870-873.

23. Lee G.-D., Wang C., Yoon E., Hwang N.-M., Kim D.-Y. and Ho K. Diffusion, coalescence, and reconstruction of vacancy defects in graphene layers Phys. Rev. Lett., 2005, V. 95, 205501.

24. Amorim R.G., Fazzio A., Antonelli A., Novaes F.D. and da Silva A.J. Divacancies in graphene and carbon nanotubes // Nano Lett., 2007, V. 7. - P. 2459–2462.

25. Kotakoski J., Krasheninnikov A. and Nordlund K. Energetics, structure, and long-range interaction of vacancy-type defects in carbon nanotubes: Atomistic simulations // Phys. Rev. B: Condens. Matter Mater. Phys., 2006, Vol. 74, 245420.

26. Liu L., Gao J., Zhang X., Yan T. and Ding F. Vacancy inter-layer migration in multi-layered graphene // Nanoscale, 2014, Vol. 6. – P. 5729-5734.

27. Kotakoski J., Krasheninnikov A., Kaiser U. and Meyer J. From Point Defects in Graphene to Two-Dimensional Amorphous Carbon // Phys. Rev. Lett., 2011, Vol. 106, 105505.

28. Kotakoski J., Meyer J.C., Kurasch S., Santos-Cottin D., Kaiser U. and Krasheninnikov A.V. // Phys. Rev. B: Condens. Mater. Phys., 2011, V. 83, 245420.

29. Yurov V.M., Guchenko S.A., Laurynas V.Ch. Surface layer thickness, surface energy and atomic volume of an element // Physico-chemical aspects of the study of clusters, nanostructures and nanomaterials, 2018, No. 10. - P. 691-699.

30. Tolman R.C. The effect of droplet size on surface tension // J. Chem. Phys., 1949, Vol. 17, № 2. - P. 333-337.

31. Rekhviashvili S.Sh., Kishtikova E.V., Karmokova R.Yu. On the calculation of the Tolman constant // Letters to ZhTP, 2007, V. 33, No. 2. – P. 1-7.

32. Peierls R. The size of a dislocation // Proc. Phys. Soc. London, 1940, Vol. 52. - P. 34–37.

33. Nabarro F.R.N. Dislocations in a simple cubic lattice // Proc. Phys. Soc. London, 1947, Vol. 59. - P. 256–272.

34. Usatenko O.V., Gorbach A.V., Kovalev A.S. Energy and Peierls barrier of the Frenkel–Kontorova dislocation (kink) // FTT, 2001, Vol. 43, issue. 7. - P. 1202-1206.

35. Grinberg B.A., Ivanov M.A., Kruglikov N.A., Antonova O.V. On the possibility of self-blocking of dislocations in various materials // Physics and Mathematics, 2009, Vol. 108, No. 1. - P. 93-104.

36. Fan T., Luo L., Ma L., Tang B., Peng L., Ding W. Study of total a-dislocations in pure magnesium based on first principles // PMT, 2014, Vol. 55, No 4. - P. 141-151.

37. Lazar M. Dislocation field theory in 2D: Application to graphene // Phys. Lett. A, 2013, Vol. 377, No 5. – P. 423-429.

38. Dettori R., Cadelano E. and Colombo L. Elastic fields and moduli in defected graphene // J. Phys.: Condens. Matter, 2012, Vol. 24, 104020.

39. Wang B., Puzyrev Y. and Pantelides S.T. Strain enhanced defect reactivity at grain boundaries in polycrystalline grapheme // Carbon, 2011, Vol. 49. – P. 3983-3988.

40. Lu J., Bao Y., Su C.L. and Loh K.P. Properties of strained structures and topological defects in graphene // ACS Nano, 2013, Vol.7. – P. 8350-8357.

41. Botello-Mernndez A.R., Declerck X., Terrones M., Terrones H. and Charlier J.-C. One-dimensional extended lines of divacancy defects in graphene // Nanoscale, 2011, V.3. – P. 2868-2872.

42. Huang H., Xu Y., Zou X., Wu J. and Duan W. Tuning thermal conduction via extended defects in graphene // Phys. Rev. B: Condens. Matter Mater. Phys., 2013, V.87, 205415.

43. Yazyev O.V. and Helm L. Defect-induced magnetism in graphene // Phys. Rev. B: Condens. Matter Mater. Phys., 2007, V.75, 125408,

44. Гринберг Б.А., Иванов М.А., Кругликов Н.А., Антонова О.В. О возможности автоблокировки дислокаций в различных материалах // ФММ, 2009, том. 108, №1. - С. 93-104.

45. Warner J.H, Margine E.R., Mukai M., Robertson A.W., Giustino F., Kirkland A.I. Dislocation-driven deformations in graphene, 2012, Science, Vol. 337. - P. 209-212.